

Quantitative Soot Measurements in an HSDI Diesel Engine

Henrik Bladh¹, Leif Hildingsson², Volker Gross³,
Anders Hultqvist⁴, Per-Erik Bengtsson⁵

1: Combustion Physics, Faculty of Engineering, Lund University, Lund, Sweden, henrik.bladh@forbrf.lth.se

2: Combustion Engines, Faculty of Engineering, Lund University, Lund, Sweden, leif.hildingsson@vok.lth.se

3: Institut für Kolbenmaschinen, University of Karlsruhe, Germany, volker.gross@ifkm.uni-karlsruhe.de

4: Combustion Engines, Faculty of Engineering, Lund University, Lund, Sweden, anders.hultqvist@vok.lth.se

5: Combustion Physics, Faculty of Engineering, Lund University, Lund, Sweden, per-erik.bengtsson@forbrf.lth.se

Abstract Quantitative in-cylinder measurements of soot volume fraction in a single-cylinder HSDI Diesel engine, based on a VOLVO D5, has been carried out using the laser-induced incandescence (LII) technique using laser excitation at 1064 nm and an ICCD camera with prompt gate detection. Quantitative data was obtained by relating the LII signal response from the engine to that from a calibration flame. The aim of this paper is twofold: to present quantitative data for relevant engine operating conditions and to discuss the issues related to quantification of the LII technique using the present approach. Two different operating condition schemes were investigated. In the first, the soot production for different amounts of EGR was investigated. The in-cylinder soot volume fraction levels were found to decrease with increasing EGR ratio in the tested EGR regime, which correlates well with engine-out soot emissions. In the second part of the investigation, the injection event was divided into one pilot injection and one main injection at a constant EGR ratio of 60%. The CAD position of the pilot injection was varied, while keeping the position of the main injection constant. Early pilot injection timings resulted in excessive fouling of the optical parts, thus limiting the accuracy of quantitative measurements. Still, the flow pattern of the soot within the cylinder is presented and discussed. The corrections needed to accurately estimate soot volume fractions in an optical engine by relating the integrated LII signal to that obtained in a calibration flame are discussed. Using a heat and mass transfer model for LII, the pressure and temperature effects on the absolute LII signals are investigated. Results show that the use of a short prompt gate (30 ns) is preferable in order to decrease systematic errors due to differences in the conditions between the engine and the calibration flame. Also the systematic errors introduced by potential particle aggregation are studied and discussed.

1. Introduction

One of the major pollutants from Diesel engine exhausts is soot, and both the health aspects and impact on the environment make it important to reduce these emissions. Soot formation is a result of incomplete combustion, which is a sign of non-optimal efficiency of the process. Increased injection pressures of modern Diesel engines may reduce total soot emissions but may on the other hand cause higher levels of particulates in the nanometer-size range, which are especially unhealthy for humans. In previous research on high speed direct injection (HSDI) Diesel engines, it has been found that soot increases with increasing exhaust gas recirculation (EGR) until a point where it suddenly falls off and approaches very low levels (Nöhre et al. 2006). This feature opens up a potential to realize a practically “zero emission” engine, however, the mechanisms behind the sudden decrease is largely unknown and considerable knowledge needs to be gained. Another important issue with modern HSDI Diesels is the calibration of pilot injection amount and timing to achieve desired combustion characteristics under low load.

In-cylinder studies of soot formation are an invaluable tool for characterizing these operating modes. One of the most promising techniques for in-cylinder measurements of soot volume fractions is laser-induced incandescence (LII), see (Santoro and Shaddix 2003) and references therein. In this technique soot particles are exposed to a rapid laser pulse, often with nanosecond duration, that heats the particles to their sublimation temperature. The increased Planck radiation from the laser-heated particles is detected and may be related to absolute soot volume fractions. The first applications of LII in IC engines were made around 1990 by Dec and co-workers (zur Loye et

al. 1990, Dec and zur Loye 1991). In these works, the usefulness of the LII method for 2-D imaging of soot volume fraction was demonstrated with efficient suppression of background luminosity and elastic scattering from liquid droplets. The LII signal was considered to be proportional to the soot concentration solely due to the theoretical study by Melton (1984). Later investigations experimentally confirmed the approximate proportionality between LII signal and soot volume fraction, see for example Quay et al. (1994) and Bengtsson and Aldén (1995).

Although these first papers on the use of LII in engines led to much information about soot formation in engines, very little attention was paid to the physical processes for laser-heated particles under these conditions as compared to those encountered in atmospheric flames. The operating conditions in IC-engines can vary over large ranges of temperatures and pressures during the engine cycle and the relationship between the signal strength and these parameters may introduce uncertainties in measurements. To improve the accuracy in quantitative soot measurements using LII, further investigations of the dependence on these parameters are needed.

One approach is to study the process using theoretical heat and mass transfer models predicting the LII signal behavior for different experimental conditions. Since the first model for laser-heated soot particles was presented in 1979 (Eckbreth 1979), there has been continuous improved understanding of the underlying physical processes of importance for LII. Much of this work was summarized in the excellent paper by Michelsen (2003). In the middle of the 90's the first experiments were published in which the time decay of time-resolved LII signals were used for particle sizing (Will et al. 1995). This development strengthened the importance of an accurate description of the heat conduction, which is the main cause for the cooling of the laser-heated particles in LII. The treatment of the heat conduction in various environments including those encountered in engines has recently been reviewed by Liu et al (2006). As soot particles are raised to temperatures around 4000K sublimation of the particles will result in heat and mass loss, a process that also is pressure dependent. The most well-known model incorporating the pressure dependence for both these processes is the one by Kock et al. (2002, 2003). This model has recently been applied for particle sizing in engines also by other groups (Bougie et al. 2006, Boiarciuc et al. 2006).

This paper presents two investigations carried out in a HSDI Diesel engine to test the influence of EGR and pilot injection timing on in-cylinder soot formation measured by LII. Quantitative data is presented, and the procedures involved in obtaining accurate data from LII signals is discussed and some systematic errors estimated using a theoretical model for the LII process recently improved for taking into account high-pressure and soot particle morphology effects.

2. Experimental

The measurements have been performed in an optically-accessible light-duty Diesel engine based on the Volvo D5, which has a displacement of 480 cm³ per cylinder (see Fig. 1). Additional engine data can be found in Table 1. Optical access was arranged through a fused silica ring that forms the upper 25 mm of the cylinder liner and also through a Bowditch-type elongated piston assembly. The optical bowl-in-piston design very closely resembles that of the all-metal production engine. With this design, parts of the bowl region can be imaged from a side view as well as from below through the piston extension. A Nd:YAG laser operating at 1064 nm was used for the laser-induced incandescence. This wavelength was chosen since it prevents interferences from polyaromatic hydrocarbon fluorescence and photo-chemical effects and also since the laser and detection wavelengths can be kept strongly separated minimizing interferences from scattering and reflections in surfaces (Vander Wal and Weiland 1994). An attenuator enabled total control of laser fluence levels without distorting the spatial beam profile of the laser energy. The near-Gaussian laser beam was formed into a 4 cm wide and 300 μm thick sheet using cylindrical lenses. Two different configurations were used in the present study and they are schematically shown in Fig. 1.

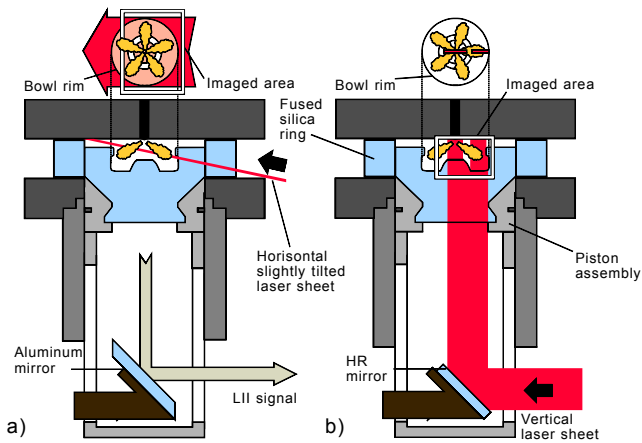


Table 1 Engine data

Bore	81 mm
Stroke	93.2 mm
Compression ratio	13.3:1
Displacement	480 cm ³ per cyl.

Fig. 1 Schematic representation of the optical engine and the two configurations used in this study. a) Imaging through the piston bowl (configuration 1), and b) imaging through the ring (configuration 2). HR = high reflectivity.

The first configuration involved detection through the piston bowl via the elongated piston (Fig. 1a). To more efficiently probe the spray volume, the optical axis was aligned slightly tilted. The second configuration involved detection from the side via the ring (Fig. 1b), and the laser was directed into the combustion chamber vertically. Due to the shape of the pip, laser light coming from the side hitting it tends to form a focus inside the fused silica material of the pip with risk of damaging it. To avoid this problem, the laser was directed into the combustion chamber via a mirror (with high reflectivity at 1064 nm) replacing the aluminum mirror inside the elongated piston assembly. While ensuring no damage, it however limited the regions that could be probed, which will be discussed below. As can be seen in Figs 1a and 1b, the sheet is dumped in the engine ceiling. This was possible without giving rise to interferences since the wavelength of the laser was in the infrared (IR) spectral region while detection was in visible/ultraviolet (UV) enabling very effective spectral filtering. The detector, a Princeton ICCD camera, was not IR sensitive thus minimizing the risk of detecting a scattered background signal. An UV fused silica lens ($f=100$ mm) was used to image the signal onto the detector. Two optical filters were used; one short-pass filter with transmission below 450 nm and one heat-absorbing Schott filter (KG3) to effectively suppress natural flame radiation and residual radiation at 1064 nm. A prompt gate with 30 ns duration was used and the laser fluence was kept at ~ 0.5 J/cm².

Calibration of the LII signals was performed using a well-characterized ethylene-air flame ($\phi=2.3$) on a McKenna burner (Axelsson et al. 2000). Soot volume fractions were established in this flame from previous extinction measurements and by using the same experimental setup when detecting the LII signal from the flame as from the engine, quantitative soot volume fractions could be evaluated from the engine data. During calibration the laser sheet was deflected from its original path and aligned into the calibration flame. The detector was moved to a position with the corresponding image plane to collect the signal. The considerations with such an external calibration approach for engine measurements, and the uncertainties and systematic errors that must be faced for estimating the soot volume fractions, is discussed in a special section of this paper.

Two different operating condition schemes were investigated; one where different amounts of exhaust gas recirculation (EGR) were used and the other where the injection timing was slightly changed. To simulate EGR, the exhaust gas from an industrial burner was cooled and led into the intake system. The EGR ratio is expressed as the engine exhaust CO₂ level divided by the engine intake CO₂ level. Three different inlet CO₂ levels were investigated in the first part, these being 3.8%, 4.3% and 4.9% intake CO₂ corresponding to 57%, 62% and 67% EGR ratio. These EGR ratios are all on the high EGR side of the soot bump, i.e. where an increasing EGR ratio gives rise to a lower engine-out soot level. A rough sketch of the soot bump is shown in Fig. 2. To get the timing of the 50% heat released at about 5 crank angle degrees (CAD) after top dead center (TDC), the start of injection (SOI) timing was altered for the different EGR ratios; this is detailed in Table 2 where a minus sign indicates a CAD position before TDC.

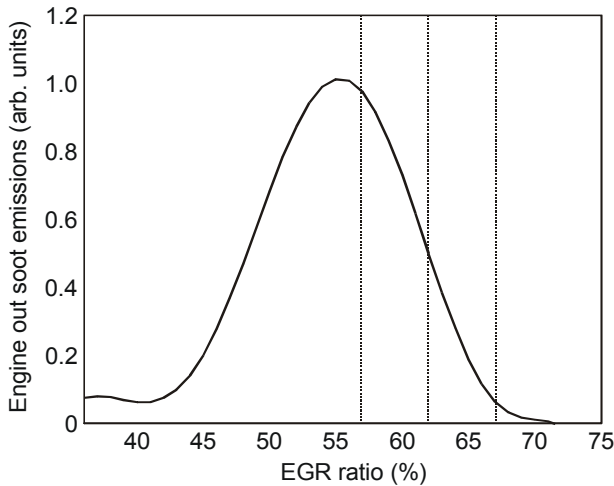


Fig. 2 Schematic plot of engine-out soot emissions as function of EGR ratio. The three operating points investigated in this work are indicated.

Table 2 EGR sweep details

Inlet CO ₂ level [%]	EGR ratio [%]	SOI [CAD ATDC]
3.8	57	-9
4.3	62	-10
4.9	67	-11

Table 3 Operating parameters for EGR sweep

Speed	1200 rpm
Load (IMEP)	2.2 bar
Inlet temperature	85 °C
Inlet pressure	1.1 bar (absolute)

Table 4 Operating parameters for change of pilot SOI

Speed	1200 rpm
SOI pilot (late)	-4 CAD
SOI pilot (early)	-7.5 CAD
SOI main	-2.2 CAD
Load (IMEP)	1.3 bar
Inlet temperature	90 °C
Inlet pressure	1.3 bar (absolute)

Other important parameters for these operating conditions are listed in Table 3. For the second part of the investigations presented here, the fuel injection event was divided into one pilot injection and one main injection, while keeping the EGR ratio constant at 60%. By changing the CAD position of the pilot injection, changes in the engine-out soot level could be measured. By phasing the pilot injection close to the main injection (late pilot injection), no soot could be detected in the exhaust, but by moving the pilot injection a little earlier (early pilot injection) some soot was detected. The main injection was always at the same location, and only the pilot SOI was changed. These measurements were conducted at quite low load to prevent excessive fouling of the optical parts. The details of these operating conditions are listed in Table 4.

3. Results from engine measurements

The fused silica piston was designed with the same basic geometry as the all-metal counterpart in the VOLVO D5 engine to facilitate realistic conditions especially inside the bowl. The sharply curved surfaces are kept to a minimum, facilitating quite large areas for imaging. The curved surfaces were strongly refractive and consequently not considered optically accessible, thus leaving gaps between areas where signals could be detected.

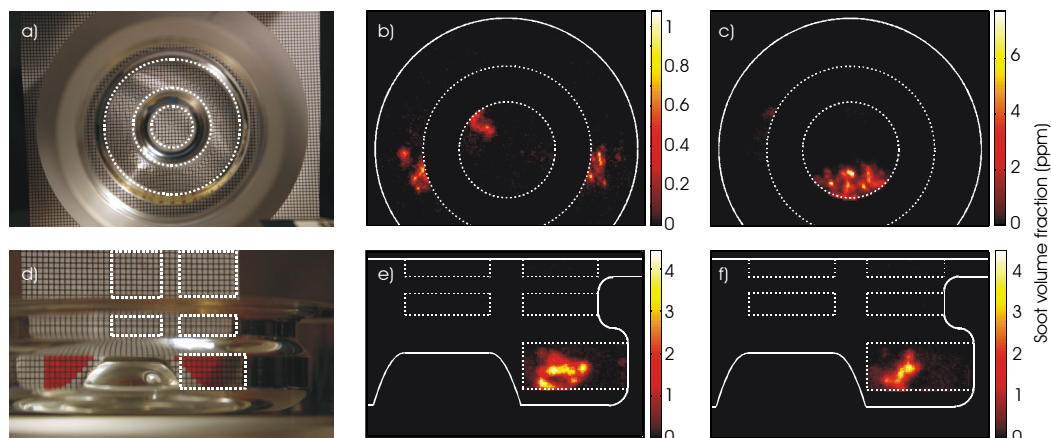


Fig. 3 The view through the optical piston for the two configurations (a and d) together with single-shot soot volume fraction images. The data in b) and c) have been obtained at 8 CAD using an EGR ratio of 57% and the images in e) and f) have been obtained at 13 CAD using late pilot injection.

To facilitate interpretation of the results presented in this paper, images of the piston are presented in Fig. 3 defining the signal areas. Two examples of soot volume fraction images are also shown. These are single-shot samples from series of 100 images per CAD. They have been compensated for detector noise levels and laser-related interferences by subtracting reference backgrounds with the laser running while motoring the engine. Quantitative data of soot volume fractions have been obtained by relating the LII signal levels to those measured in the calibration flame.

3.1. Effect of EGR

In a first study, three different levels of EGR are tested by adding exhaust gas from a burner for domestic heating so that the intake charge consisted of 3.8%, 4.3% and 5.0% CO₂, corresponding to 57%, 62% and 67% EGR. As previously mentioned, these operating points are on the right side of the soot bump as illustrated in Fig. 2. From the heat release analysis in Fig. 4 it is clear that the peak heat release diminishes with increasing EGR. This is expected due to less available oxygen at higher EGR levels. The increased ignition delay, brought on by the increased EGR amount was counteracted by advancing the injection timing so as to keep the crank angle of 50% burnt at the same position, 5 CAD after TDC. The higher rate of heat release in combination with lower heat capacity of the gas at low CO₂ concentrations yields higher flame temperatures for a given equivalence ratio which in turn translates into higher amounts of soot in the exhaust. In the studied cases, the decreasing temperature has stronger effect on the soot development than the increasing equivalence ratio so the net result is decreasing engine-out soot emissions with increasing amount of EGR.

In the average soot development, as displayed in Fig. 4, the difference

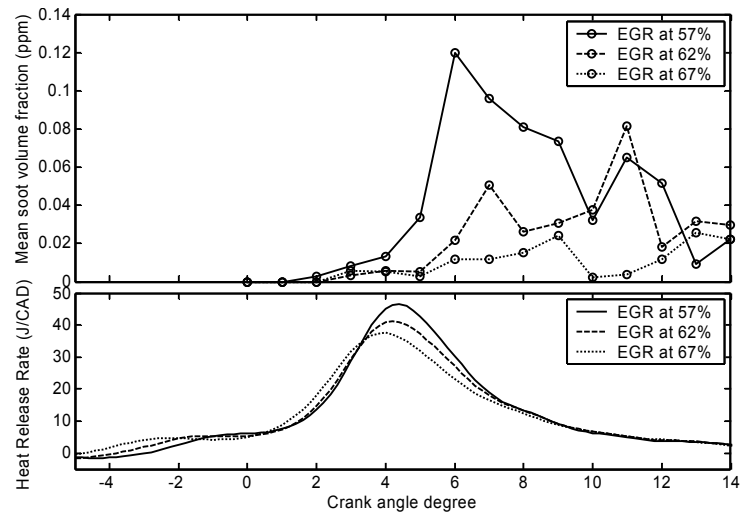


Fig. 4 Soot development defined as cycle- and spatially averaged volume fractions and calculated heat release rates for EGR ratios of 57, 62 and 67% respectively.

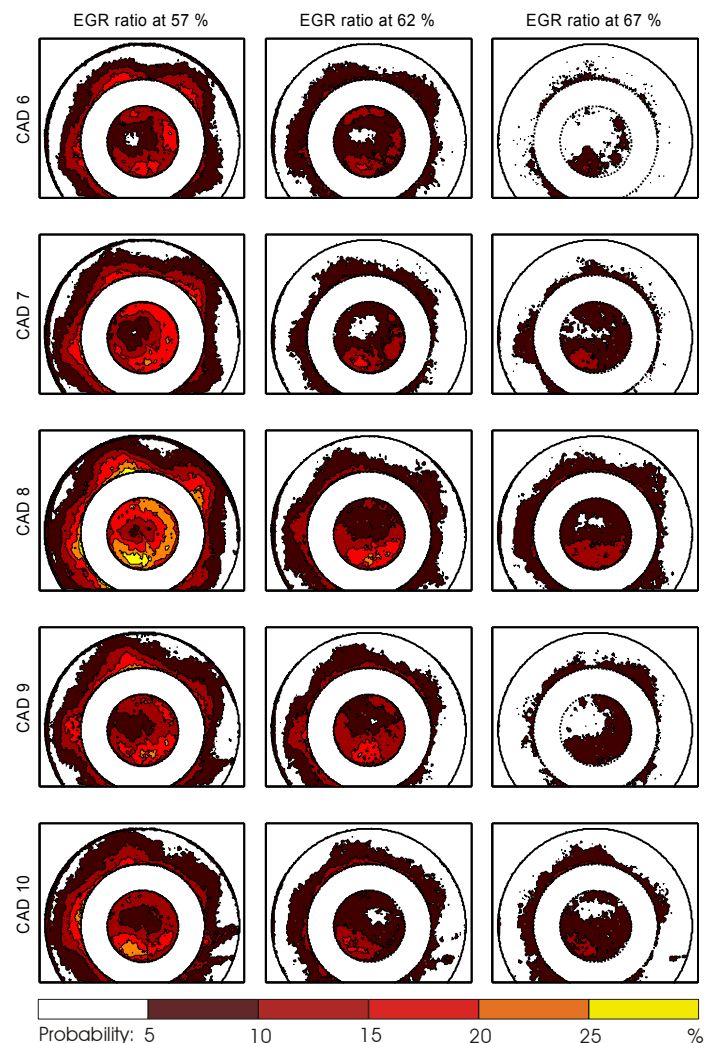


Fig. 5 Probability density distribution for the three different EGR levels as function of crank angle degree. The contours represent the probability of obtaining a soot volume fraction above 0.02 ppm and is specified in the color bar. Probability higher than 25% is marked yellow.

between the three cases is significant. Especially, the low EGR case (57%) has high peak soot concentration and also subsequent strong oxidation. Even though there are some discrepancies in the later part of the soot history, the overall trend is towards lower soot concentration after the initial peak. The high EGR case (67%) on the contrary only shows slow formation with virtually no apparent soot oxidation. Surprisingly all the three cases converge to very low concentrations of soot.

The map in Fig. 5 shows the probability density distributions of the soot volume fraction at the three different EGR levels as function of crank angle. In all cases the spray directions can be identified. The soot is concentrated to the central parts of the bowl, probably a result of the very modest load. With increasing EGR the occurrence of soot becomes more and more scarce and for the highest EGR ratio the soot appears very stochastically at central parts.

3.2. Effects of pilot injection timing

The second investigation is dealing with the in-cylinder soot volume fraction dependence on the pilot injection timing. Comparing the heat release rates of the two cases (see Fig. 6), reveals the significant difference that the early pilot seems to ignite and give off some heat before the main heat release occurs. This is not the case for the late pilot which seems to be fully integrated with the main heat release. For the “early pilot”-case, this should result in higher gas temperatures at the SOI for the main injection event, thus advancing the heat release significantly. However, in the sequences of probability density distributions shown in Fig. 7, there are rather large differences in where and when soot appears. Especially in the center section above the pip, the “early pilot”-case shows significant amounts

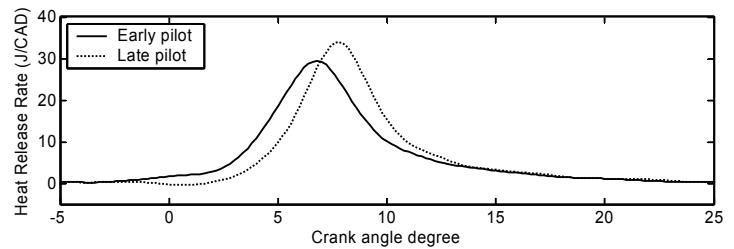


Fig. 6 Heat release rates for two test cases with varying pilot SOI.

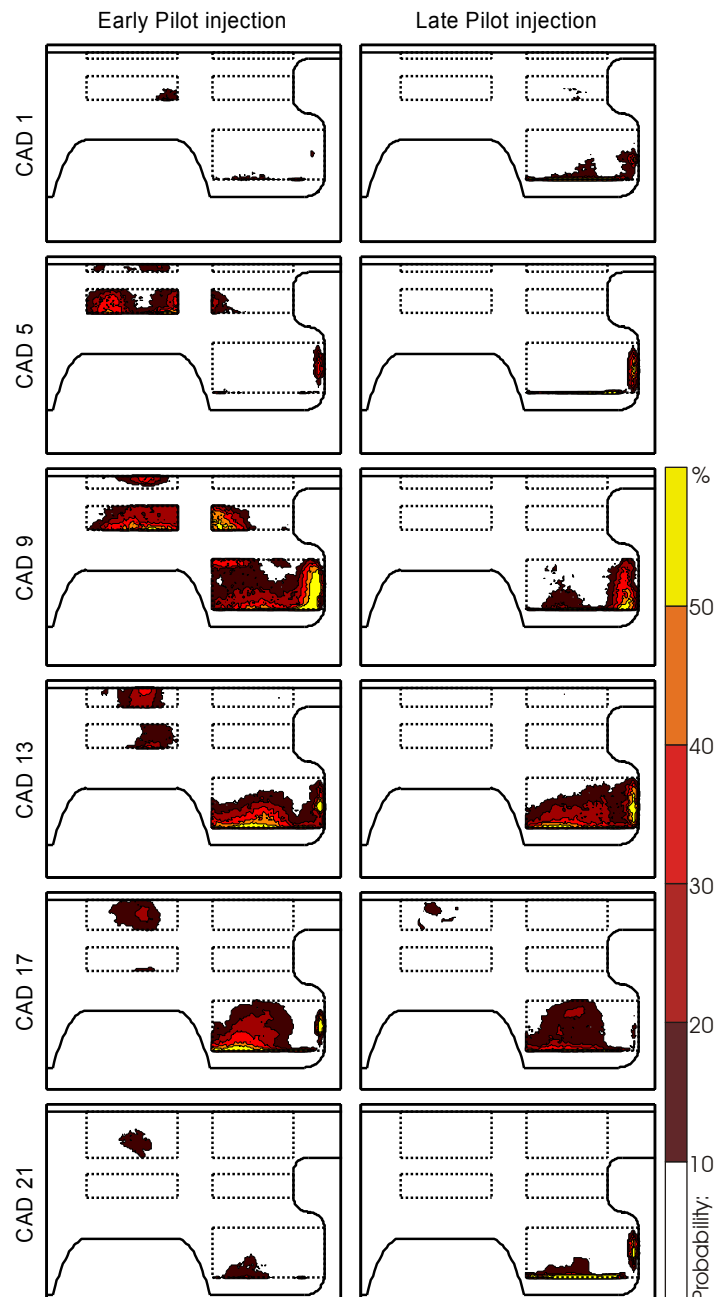


Fig. 7 Probability density distribution for the two tested cases with different pilot SOI as function of CAD. The contours represent the probability of obtaining a soot volume fraction above 0.1 ppm and is specified in the color bar. Probability higher than 50% is yellow.

of soot. This central soot cloud seems to prevail in the same location mostly affected by oxidation and only to a minor extent transported by convection to other parts of the bowl. Obviously, fluid motion is needed to transport unused oxygen to this part of the combustion chamber, alternatively to transport the soot to regions with oxygen, in order for the oxidation to proceed. In contrast, in the bowl area where the swirling motion might sweep the soot cloud in and out of the measurement plane the measurement is harder to interpret. Apart from the central part, the soot occurrence from the “early pilot” and “late pilot” are very similar from 9 CAD throughout the cycle. This indicates that the slightly elevated engine-out soot level for the early injection case could be due to soot from the central region of the cylinder that has not oxidized. While difficult to say without other types of measurements, it is probable that the central region contains little oxygen after combustion at this high EGR ratio. For this case, where there seems to be only very weak flow structures that could mix the fluid in the central region with fluid from regions containing unused oxygen, it is probable that the soot oxidation rate is limited. The major soot cloud resides in the bottom of the bowl where it is convected in a clockwise motion setup by the injection event, agreeing with prior findings by the authors (Hildingsson et al. 2006). At about 23 CAD there is very little soot left to detect. On an average, the maximum soot level found inside the combustion chamber at later crank angles, after main heat release, correlates well with preliminary engine-out emissions.

For early pilot injection, soot production appeared to be stronger as compared to late timing. This is however not evident when comparing the probability density distributions of soot volume fraction in Fig. 7, where both cases show similar probability levels. The most probable reason is the excessive soot deposits on the interior of the piston bowl, which were obtained for the case with early pilot, effectively decreasing the measured LII signal. This problem was not encountered for late injection. Due to this difference, no absolute comparison of probabilities between the two cases is intended.

4. Quantification aspects

The aim of this section is to discuss the considerations involved in successfully obtaining quantitative soot volume fractions from in-cylinder measurements using the laser-induced incandescence technique. The first and foremost use of the formed knowledge base is to determine the experimental conditions giving lowest systematic errors in measured in-cylinder soot volume fraction. The knowledge base may also be used during the data evaluation process for compensating for effects that cannot be overcome simply by experimental design considerations.

The LII measurements presented in this work has been calibrated for absolute soot volume fraction using a calibration flame operated at atmospheric pressure. While enabling a stable well-characterized reference for the engine setup, many uncertainties should be considered. These may be divided in two major groups. (1) The calibration burner and the engine combustion chamber are located at two different positions in the laboratory, and (2) the two systems have different global environments (pressure, temperature) and possibly also different properties of soot. The first point will be briefly addressed while focus will be on the second.

The fact that the calibration flame and the measurement region in the engine are located at different positions must be considered. The laser sheet has to be deflected from its original path into the engine and instead be directed through the flame. A difference between these two cases is that the measurement volume in the engine combustion chamber is located behind thick curved optical windows. These windows result in (1) laser beam energy loss, (2) laser beam distortion due to curved surfaces, (3) image plane distortion due to curved surfaces, and (4) enable soot deposit buildup, which effectively obstructs the LII signal on its way to the detector. Another group of uncertainties arise due to attenuation of local laser fluence along the measurement volume length due to absorption from the soot itself, and so called signal trapping effects, i.e. attenuation of the LII signal due to absorption in (non-deposited) soot on its way to the detector.

The inaccuracy introduced by all these effects will be dependent on the individual uncertainties to different degree, often in a non-linear manner. This has to do with both the energy dependence of the LII signal and the LII signal dependence on soot volume fraction. The energy dependence of the LII signal is usually denoted the fluence curve. When conducting soot volume fraction measurements with LII it is customary to choose laser fluence in the moderate-high fluence regime ($\sim 0.3 - 0.6 \text{ J/cm}^2$) to ensure low dependence of the LII signal on laser fluence (Vander Wal and Jensen 1998). This would ensure that unavoidable changes of the laser sheet characteristics caused by the optical parts of the engine only would introduce minor errors in the measurements. In this work a laser fluence of $\sim 0.5 \text{ J/cm}^2$ was chosen since tests performed in the calibration burner verified only moderate energy dependence in this region. This ensured that uncertainties in local laser fluence only mildly influenced the final uncertainty in detected LII signal levels.

When using a horizontally aligned laser sheet for engine measurements via a cylindrically shaped access window, a lens effect will be introduced. The laser sheet will diverge and become somewhat wider. This will effectively decrease the local laser fluence. In addition, reflections in surfaces and possible impurities in the optical parts will decrease the true in-cylinder laser fluence from its original value. Tests performed before measurements proved the uncertainties to be less than 5% within the measurement volume and keeping in mind the only moderate fluence dependence, this effect on the LII signal is estimated to be below 1%. A much more severe problem due to its dependence on local soot concentrations is attenuation of the laser beam inside the combustion chamber due to the presence of soot. Measurements in homogeneous concentrations sometimes enable compensation for such absorption effects, but the extremely stochastic signals achieved under the conditions in this work precluded such procedures. The weak energy dependence of the LII signal in the operating fluence region do however minimize also this effect, and since the measurement clearly showed very small soot clouds, the LII signal uncertainty due to absorption effects is estimated to less than 3%. The signal that originates from the measurement volume inside the combustion chamber will also suffer from attenuation and deflection effects on its way to the detector. Tests showed that the signal was attenuated by $\sim 6\%$ due to the optical parts. Another effect is signal trapping, i.e. the LII signal gets partly absorbed by other soot particles on its way to the detector. This effect may be large but is, as the case for laser beam absorption, not easily corrected for without additional measurements. In addition, the signal loss due to absorption in soot deposits on the optical parts must be considered. Such deposits introduce significant errors, and indeed prevented accurate quantification of the early pilot injection data presented in this paper. A rough compensation for the effects of signal loss due to trapping and deposits is in principle possible by using an online laser absorption setup recording the fraction of light absorbed through both cylinder and bowl area during an engine test run as function of CAD (Boiarciuc et al. 2006).

We conclude this discussion by noting that several of the effects, if not compensated for, will give systematic errors contributing in the same direction, i.e. underpredicting the signal in the engine as compared to the calibration flame. Though some of the effects may need additional measurements to ensure accurate compensation, many of the effects can be compensated for in a relatively straightforward way.

Basically all aforementioned effects are related to the characteristics of transmission, refraction and absorption of in- and outgoing light. In the upcoming discussion, focus will be on the LII process itself and the interaction between the laser pulse and the soot particles in the measurement volume. The LII technique is based on rapid heating of soot particles with a short laser pulse giving rise to the increased Planck radiation detected as the LII signal. While principally straight-forward, the exact dependence between experimental parameters like laser energy, spatial and temporal distribution of laser energy, gas pressure and temperature, size distribution of particles etc. is extremely complex and to large extent still uncertain. To help understand the dependencies and to be used as a tool during data evaluation, physical models have been developed to predict the LII signals from the heated soot particles during specified experimental conditions. To study the effects

of the global environment and the soot properties in the measurement volume, such a model will be used to highlight and at least roughly quantify possible uncertainties relevant for engine diagnostics using the present calibration scheme.

The model used in this work is basically described in (Bladh et al. 2004) and some modifications are discussed in (Bladh et al. 2006). It is based on time-dependent heat and mass balance equations derived for spherical soot particles of predefined characteristics. For the present task, the model has been improved to include high-pressure and soot aggregation effects. To account for heat conduction in both the transition and the continuum regimes the Fuchs heat transfer model proposed by Filippov et al. (2000) has been used. For the same reason the sublimation term used in (Bladh et al. 2004) has been extended with a second term for the continuum regime (Hofeldt 1993, Snelling et al. 2000). Additionally a simple empirical relation has been incorporated to account for the reduced surface-to-volume ratio for soot particles that become aggregated (Liu et al. 2005). The laser energy, fluence, wavelength, sheet width and thickness were defined according to the experimental conditions. The spatial distribution of laser energy was assumed Gaussian in width and uniform in height. A Gaussian temporal profile was assumed with the FWHM specified by the laser manufacturer (9 ns). The detection wavelength interval was determined by the filter characteristics and detector sensitivity. The absorption function $E(m)$ was set to 0.293 (Bladh et al. 2006).

The temperature and pressure data from one measurement series presented in this paper is shown in Fig. 8. As can be seen the pressure varies in the range 30 – 50 bar, and the temperature in the range 800 – 1200 K. The calibration flame is operated at atmospheric pressure and based on the characterization of similar flames using rotational CARS (Vestin et al. 2005) the temperature has been estimated to 1700K at the reference location. Before presenting an estimation of uncertainties in evaluated soot volume fraction for the difference in operating conditions for the calibration flame and the engine, an investigation of signal dependencies when only varying single parameters is shown in Fig. 9.

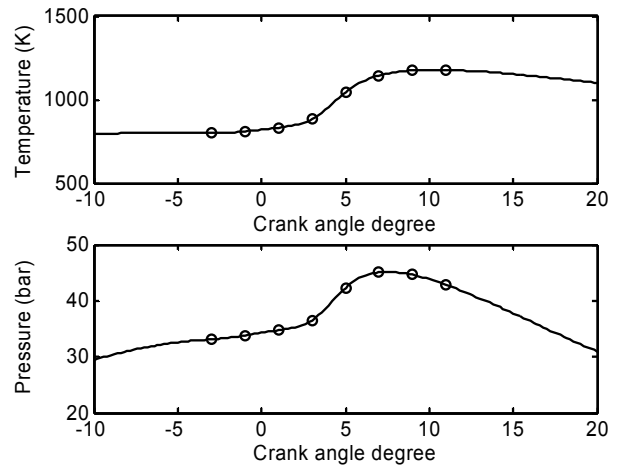


Fig. 8 Cycle-averaged in-cylinder pressure and temperature for the 57% EGR series. The markers denote the exact crank angle positions for the LII measurements.

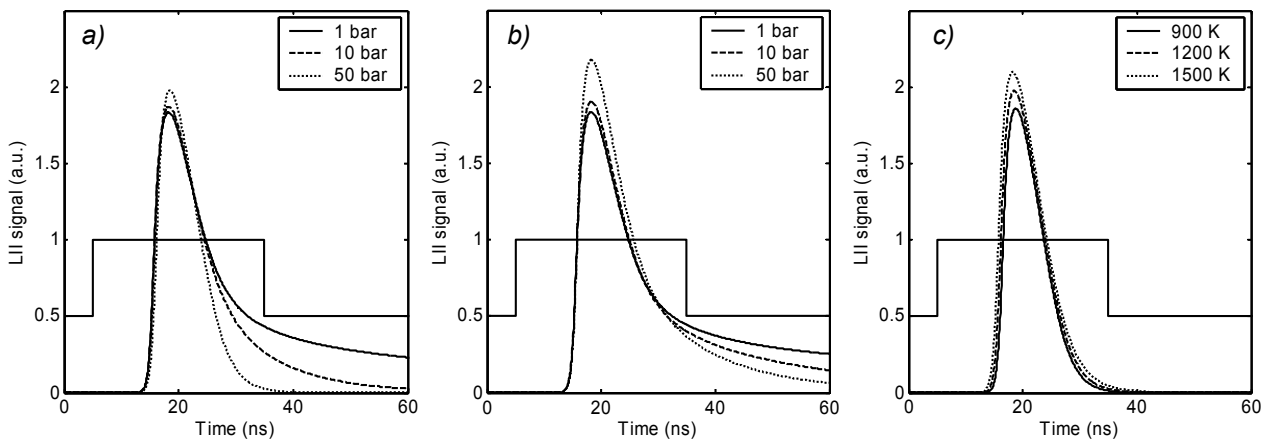


Fig. 9 Modeled time-resolved LII signals for different gas pressures and temperatures. All cases are derived using the laser fluence (0.5 J/cm^2), a Gaussian laser sheet and primary particle diameter of 30 nm. In a) the pressure is varied for isolated soot particles while keeping the temperature at 1200 K. In b) the pressure is varied for soot particles modeled as aggregates with $N_p=500$ (N_p is the number of particles per aggregate) and $T=1200 \text{ K}$. Finally in c) a case is shown for a pressure of 50 bar and isolated particles, where the temperature has been varied. The 30 ns detector gate is indicated.

Figure 9a shows a case where the gas temperature is held constant at 1200K and the pressure is varied ranging from atmospheric to high pressures relevant for engine measurements. The soot particles are assumed to be isolated and 30 nm in diameter. While the peak LII signal seems relatively unaffected by the pressure variation, the decay is drastically shortened. This is consistent with the findings by Hofmann et al. (2003).

The most pressure-dependent process in the model is the heat conduction, which scales approximately linearly with gas pressure. The particles will cool much faster at high pressure conditions than at ambient conditions since the collision frequency between soot particles and molecules increases. It is obvious that a long gate width increases the LII signal dependence on pressure. The error would be expected to be significantly larger if the prompt signal is avoided altogether, so called delayed gating. This detection mode ideally has the great potential of reducing interferences from other processes like Mie scattering of droplets and laser-induced fluorescence. However, one has to keep in mind the pressure dependence, and especially the fact that the decay time of LII signals from smaller particles (5-10 nm) may be undetectable due to their extremely short decay.

In Fig. 9b is shown the results from the same conditions as in a) except that the soot particles are assumed to be aggregated. The peak signal is predicted to increase with pressure to a higher degree than for isolated particles. This is believed to be due to the heat transfer being weakened as aggregation is decreasing the efficiency of cooling by reducing the available surface area. The pressure dependence of the decay will remain, but will be weakened, and since the peak signal is not constant, the contribution of pressure to the integrated signal is actually being counteracted by the effect of aggregation.

In Fig. 9c is shown a case where the pressure is constant at 50 bar while varying the gas temperature. This parameter also seems to influence the LII signal for the prompt signal. This can be understood if considering the heating effect. The gas temperature determines how much laser fluence would be needed to heat the soot particles to the vaporization temperature of soot, at which LII normally is operated. In low temperature environments, more laser energy will be needed to heat the particles than in a high temperature environment. Since the laser fluence is held constant, a relatively strong dependence is noticeable. It may at first be unexpected that the peak LII signal varies at all since the fluence is quite high (0.5 J/cm^2). However, one must keep in mind that these results are derived for a non-uniform spatial profile of the laser, and hence many soot particles in the spatial wings of the beam are only heated to moderate temperatures.

To estimate the systematic errors introduced from these effects on a typical data set presented in this paper, time-resolved LII signals were modeled for the temperatures and pressures recorded for the 57% EGR-ratio data shown in Fig. 8. Knowledge of aggregation inside the engine is limited and therefore two test cases were designed where one assumes no aggregation and aggregation with 500 primary particles per aggregate ($N_p=500$), respectively. LII signals were also modeled for the conditions present in the calibration flame, conditions well-known from previous studies. In Fig. 10 the relative difference (corresponding to a systematic error) is shown in time-gated LII signal for the modeled cases along the crank angle degrees measured in the EGR 57% series due to the difference in temperature and pressure between engine and reference flame. As could be seen from Fig. 10 the systematic error can be substantial at long detection gates, where much of the signal decay is collected, and early CAD's (where the temperature is low) – especially for the case with no aggregation. In principle the results in Fig. 10 could be used to compensate the measured data for these effects, but one should keep in mind that large uncertainties exist in the parameters of these modeled test cases. The knowledge of the morphology of the engine soot is not readily available, the particle size distribution is not known and the predicted errors will, due to its coupling to the gas temperature effect, rely on the exact laser fluence used – just to mention some uncertain parameters. The validity of the model at these high-pressure conditions, especially for correctly treating the sublimation process is also unclear. We intend to pursue such investigations in future work.

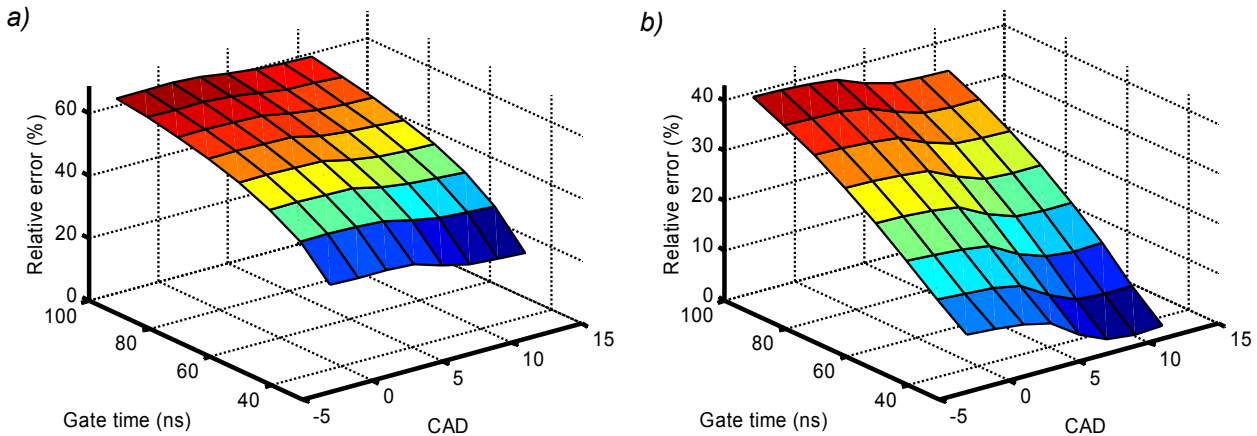


Fig. 10 Relative errors due to difference in temperature and pressure between engine and calibration flame as function of crank angle degree position for the EGR 57% series and detector gate width. a) No aggregation assumed, b) aggregation assumed with $N_p=500$. Note that the relative error is defined as positive when the signal level in the engine is lower than the corresponding signal in the flame.

5. Conclusions

In-cylinder soot volume fractions have been measured in a HSDI Diesel engine with realistic combustion chamber geometry using the laser-induced incandescence technique. The use of 1064 nm excitation combined with short-pass detection below 450 nm proved to very efficiently reduce problems with laser-induced interferences. The soot volume fraction dependence on the EGR ratio was investigated and showed that most soot production during combustion, at least at high ratios, seems to take place after the peak in the rate of heat release. While the soot history, during one cycle, look rather different for the three investigated EGR levels, they converge to more or less the same level after the main combustion. Investigating early and late pilot injection, the main difference in the soot occurrence is that soot is present in the centre of the cylinder, above the pip, in the early pilot injection case whereas no soot is detected in this position for the late injection case. Finally the issues related to quantification of the LII signal in terms of soot volume fractions were discussed. Systematic errors in quantification due to the LII signal dependence on gas temperature and pressure were predicted theoretically for different choices of experimental parameters and soot properties and it was concluded that short prompt detection would minimize the effects on the results.

6. Acknowledgements

This work has been performed within the project GenDies financed by the Center for Combustion Science and Technology (CECOST) through the Swedish Energy Agency and Volvo Car Corporation. The authors want to thank the financial sponsors and the staff in the engine laboratory.

7. References

- Axelsson B, Collin R, Bengtsson P-E (2000) Laser-induced incandescence for soot particle size measurements in premixed flat flames. *Appl Opt* 39:3683-3690
- Bengtsson P-E, Aldén M (1995) Soot-visualization strategies using laser techniques: Laser-induced fluorescence in C_2 from laser-vaporized soot and laser-induced soot incandescence. *Appl Phys B* 60:51-59
- Bladh H, Bengtsson P-E (2004) Characteristics of laser-induced incandescence from soot in studies of a time-dependent heat- and mass-transfer model. *Appl Phys B* 78:241-248

- Bladh, H, Bengtsson P-E, Delhay J, Bouvier Y, Therssen E, Desgroux P (2006) Experimental and theoretical comparison of spatially resolved laser-induced incandescence (LII) signals of soot in backward and right-angle configuration. *Appl Phys B* 83:423-433
- Boiarciuc A, Foucher F, Mounaim-Rousselle C (2006) Soot volume fractions and primary particle size estimate by means of the simultaneous two-color-time-resolved and 2D laser-induced incandescence. *Appl Phys B* 83:413-421
- Bougie B, Ganippa L C, Dam N J, Ter Meulen J J (2006) On particulate characterization in a heavy-duty diesel engine by time-resolved laser-induced incandescence. *Appl Phys B* 83:477-485
- Dec J, zur Loye A O (1991) Soot distribution in a D.I. Diesel engine using 2-D laser-induced incandescence imaging. SAE Paper 910224
- Eckbreth A C (1979) Effects of laser-modulated particle incandescence on Raman scattering diagnostics. *J of Appl Phys* 48:4473-4479
- Filippov A V, Rosner D E (2000) Energy transfer between an aerosol particle and gas at high temperature ratios in the Knudsen transition regime. *Int J Heat Mass Transf* 43:127-138
- Hildingsson L, Hultqvist A, Miles P (2006) The effect of swirl and injection phasing on flow structures and mixing in an HSDI diesel engine. To be presented at THIESEL 2006, Valencia, Spain
- Hofeldt, D L (1993) Real-time soot concentration measurement technique for engine exhaust streams. SAE paper 930079
- Hofmann M, Bessler W G, Schulz C, Jander H (2003) Laser-induced incandescence for soot diagnostics at high pressures. *Appl Opt* 42:2052-2062
- Kock B F, Eckhart T, Roth P (2002) In-cylinder sizing of Diesel particles by time-resolved laser-induced incandescence (TR-LII). *Proc Comb Inst* 29:2775-2781
- Kock B F, Roth P (2003) Two-color TR-LII applied to in-cylinder Diesel particle sizing. *Proc Eur Combust Meet*
- Liu F, Smallwood G J, Snelling D R (2005) Effects of primary particle diameter and aggregate size distribution on the temperature of soot particles heated by pulsed lasers. *Quant. Spectrosc. Radiat. Transfer* 93:301-312
- Liu F, Daun K J, Snelling D R, Smallwood G J (2006) Heat conduction from a spherical nano-particle: status of modeling heat conduction in laser-induced incandescence. *Appl. Phys. B* 83:355-382
- zur Loye A O, Siebers D L, Dec J E (1990) 2-D soot imaging in a direct-injection Diesel engine using laser-induced incandescence. *COMODIA* 90:523-528
- Melton L A (1984) Soot diagnostics based on laser heating. *App Opt* 23:2201-2208
- Michelsen H A (2003) Understanding and predicting the temporal response of laser-induced incandescence from carbonaceous particles. *J Chem Phys* 118:7012-7045
- Nöhre C, Andersson M, Johansson B, Hultqvist A (2006) Characterization of partially premixed combustion. Submitted to SAE Powertrain and Fluid Systems, Toronto
- Quay B, Lee T-W, Ni T, Santoro R J (1994) Spatially resolved measurements of soot volume fraction using laser-induced incandescence. *Combustion and Flame* 97:384-392
- Santoro R J, Shaddix C R (2002) Laser-induced Incandescence. In *Applied Combustion Diagnostics*, ed. by K Kohse-Höinghaus, J.B. Jeffries, (Taylor & Francis, London 2002) pp. 252-286
- Snelling, D R, Liu F, Smallwood G J, Gülder, Ö L (2000) Evaluation of the nanoscale heat and mass transfer model of LII: Prediction of the excitation intensity. *Proceedings of the 34th National Heat Transfer Conference*, Paper 12132
- Vander Wal R L, Weiland K J (1994) Laser-induced incandescence: Development and characterization towards a measurement of soot-volume fraction. *Appl Phys B* 59:445-452
- Vander Wal R L, Jensen K A (1998) Laser-induced incandescence: Excitation intensity. *Appl Opt* 37:1607-1616
- Vestin F, Afzelius M, Brackmann C, Bengtsson P-E (2005) Dual-broadband rotational CARS thermometry in the product gas of hydrocarbon flames. *Proc Combust Inst* 30:1673-1680
- Will S, Schraml S, Leipertz A (1995) Two-dimensional soot-particle sizing by time-resolved laser-induced incandescence. *Opt Lett* 20:2342-2344